Investigation of Freejets Issued from Small Solid-Propellant Rocket Engines

J. Allègre* and M. Raffin*
Société d'Etudes et de Services pour Souffleries et Installations Aérothermodynamiques, Paris, France
and
J. -C. Lengrand†
Laboratoire d'Aérothermique du Centre National de la Recherche Scientifique, Meudon, France

Pilot probe and electron beam measurements have been performed in the plumes exhausting from small solid-propellant rocket engines into a low-density atmosphere. Results indicate freezing of the vibrational energy and consistency of the data with a jet model previously proposed by the authors. Two parameters introduced in the interpretation of electron beam data must have been fitted, but their final values do not differ greatly from predictions based on their physical meaning.

Nomenclature

c = mole fraction
$f(\theta)$ = angular density distribution
i = electron beam intensity
i_c = intensity collected by the Faraday cup
I = intensity of gas fluorescence
k = characterizes the sensitivity of the detection system
m = defined in Eq. (5)
M = Mach number
n = total number density of the gas mixture
n_i, n_j = number densities of gases i and j, respectively
$n(i,j)$ = characterizes the quenching of gas i emission by molecules of type j
p = pressure
p_s = nozzle wall pressure, near from exit section
p_t = impact pressure
Q = overall quenching density defined in the text
r = radius, or distance from nozzle
r_{MD} = Mach disk distance
Re = Reynolds number
T = temperature
X = abscissa along jet axis
Y = distance from jet axis
α_i = proportional to the emission cross section of gas i at the considered wavelength when excited by high energy electrons
γ = specific heat ratio
ϕ = diameter
μ = viscosity
θ = polar angle
θ_∞ = direction of the outermost streamline in the absence of nozzle boundary layer and for zero background pressure

Subscripts

c = nozzle critical section
e = nozzle exit section
i,j = gases i and j, respectively
w = nozzle wall
o = nozzle stagnation conditions

Submitted Nov. 19, 1982; revision received Aug. 12, 1983.

*Research Engineer.
†Research Scientist.

Introduction

THE present work was performed in order to test the possibility of using the electron beam fluorescence technique for probing the exhaust plume from a solid-propellant rocket engine and to compare the results obtained to those given by a simple model of underexpanded jets.[1]

Experiment

Twenty-four small, solid-propellant rocket engines were fired in the SR3 vacuum facility of the Laboratoire d'Aérothermique at Meudon. Only six thrusters were built, each one being used four times. Between successive runs the thrusters were cleaned, their geometrical characteristics were verified, and they were equipped with a new propellant grain. All these thrusters were identical. The diameter of the nozzle throat was $\phi_c = 1.9$ mm and the diameter of the nozzle exit section was $\phi_e = 9.27$ mm. The diverging part of the nozzle was conical, with a 15-deg half-angle.

The thrusters were designed to provide nearly constant combustion chamber pressure (typically $p_o = 16$ bars). From propellant composition, the manufacturer estimated the combustion chamber temperature ($T_o = 2400$ K) and the exhaust-gas composition under combustion chamber conditions (Table 1). The specific heat ratio γ could thus be estimated equal to 1.375 under the assumption of total freezing of vibrational energy and approximately 1.32 under the assumption of total vibrational equilibrium. An alternative gas composition, based on the hypothesis of chemical equilibrium up to the nozzle section with area ratio $A/A_c = 9$ yielded somewhat higher specific heat ratios (1.382 for frozen vibrational energy). For both compositions the molecular weight was 23.2 g/mole.

Pressure inside the vacuum chamber (jet background pressure) progressively increased during the run,and could usually be maintained lower than 0.12 Torr, thus providing proper working conditions for the electron gun. Typical test duration was 20 s.

A 20 keV electron beam was passed through the plume. The image of the beam was formed in the plane of a rectangular slit through an optical system consisting essentially of a lens

and a mirror (Fig. 1). The position and the size of the slit thus delimitated the volume from which luminescence was measured. The light was led by fiber optics located outside the vacuum chamber, and its intensity was recorded. An interference filter was placed just ahead of the photomultiplier in order to select the wavelength range corresponding to the N_2 first negative system (0-0) vibrational band. The extremities of the fiber optics had rectangular sections larger than the slit. All the light passing through the slit was thus collected. A preliminary calibration of the photomultiplier response versus local gas density was performed by varying the air pressure inside the vacuum chamber before each run. Because of the self-emission of the exhaust gas, the electron beam was switched off a few seconds after the beginning of the test, and the resulting decrease of light intensity was interpreted as the intensity of the beam-induced fluorescence.

A Pitot probe was placed at another location in the flow field and the impact pressure was recorded. Neither the electron beam nor the Pitot probe were displaced within the duration of a run. They were moved between the runs in order to investigate the flow field range $50 \leq X/r_c \leq 200$ and $0 \leq Y/r_c \leq 50$.

Four other quantities were monitored during the test: combustion chamber pressure p_o, background pressure, electron beam intensity i_c collected by a Faraday cup, and the pressure p_s measured through a small hole in the nozzle wall 1 mm upstream of the nozzle exit plane. Both p_o and p_s were measured by strain gage transducers. The background pressure was measured by a Datametrics variable capacitance transducer. The impact pressure was measured by a Pace variable reluctance transducer.

Nozzle Flow

Nozzle exit conditions have been determined by a boundary layer calculation based on the integral method described in Ref. 2. The viscosity of the exhausting gas mixture was calculated according to Ref. 3. The uncertainty in gas composition appeared to have negligible influence on the viscosity-temperature law that could be fitted within 5% by

$$\mu = 2.36 \times 10^{-7}\, T^{0.736} \tag{1}$$

in the range 300 K < T < 2400 K (μ is in kg $s^{-1} m^{-1}$ and T in Kelvin).

The Prandtl number was taken constant and equal to a value of 0.42, which was deduced from the thermal properties of the gases under consideration at room temperature. The nozzle wall temperature T_w was taken equal to 1000 K, roughly halfway between room temperature and recovery temperature of the flowing gas. Stagnation chamber pressure was taken equal to 16 bars.

The critical parameter of the boundary layer calculation is the specific heat ratio. The flow in the nozzle was calculated for different constant values of γ. The resulting nozzle wall pressure p_s at the location where pressure was measured during the experiments, and the nozzle exit Mach number M_e, are plotted in Fig. 2 against γ. The wall pressure p_s has been nondimensionalized by the combustion chamber pressure p_o. An additional nozzle flow calculation was performed for $\gamma = 1.37$ under the hypothesis of adiabatic nozzle wall, and the corresponding results are plotted as circles in Fig. 2.

The measured values of p_s and p_o varied during each run and from one run to another. The ratio p_s/p_o has also been plotted in Fig. 2. Each bar indicates the minimum and the maximum value for a given run. In order to retain only steady-state values, the pressures recorded during the first 3 and the last 3 seconds of each run were discarded.

It appears in Fig. 2 that the measured values of p_s/p_o are consistent with values of γ in the range 1.36-1.38. This indicates total or nearly total freezing of vibrational energy. A more precise information relative to γ would be difficult to obtain because of experimental data scatter and uncertainty in nozzle wall temperature.

Specific heat ratio $\gamma = 1.37$ and exit Mach number $M_e = 4.6$ were introduced in the jet model for comparison with experimental Pitot probe and electron beam data. These values correspond to a nozzle critical Reynolds number $Re_c = 3.46 \times 10^4$ (based on throat diameter) and a mass-flow rate of 3.31 g/s. The boundary layer displacement thickness in the nozzle exit plane is equal to 0.077 times the nozzle exit radius r_e.

Jet Model

A semiempirical expression for density distribution in a freejet exhausting from a sonic or supersonic nozzle into a low-pressure atmosphere has been given by the present authors in Ref. 1 and may be rewritten as

$$n/n_o = 0.439\{(\gamma-1)/2\}^{-0.378}$$

$$\{\theta_\infty/(\pi/2)\}^{-1.92}(r/r_c)^{-2} f(\theta) \tag{2}$$

where $f(\theta)$ is the angular density distribution given by Boynton[4]

$$f(\theta) = \{\cos[(\pi/2)(\theta/\theta_\infty)]\}^{2/(\gamma-1)} \tag{3}$$

This description is only valid in the central part of the jet, i.e., on the streamlines originating from the isentropic core of the nozzle flow. Furthermore, it is restricted to that part of the jet which is not influenced by background pressure, i.e., upstream of the barrel shock and of the Mach disk. The Mach disk distance r_{MD} was calculated using the expression given in Ref. 1 for a background pressure of 0.1 Torr. It was found that the Mach disk was far downstream of the region under investigation ($r_{MD} = 920 r_c$).

From the above density distribution, the Mach number distribution within the jet may be easily deduced by the

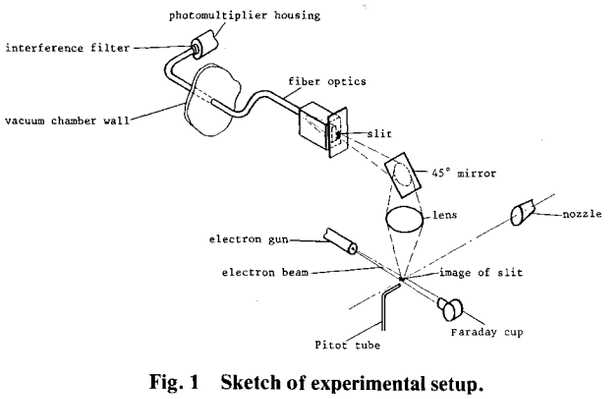

Fig. 1 Sketch of experimental setup.

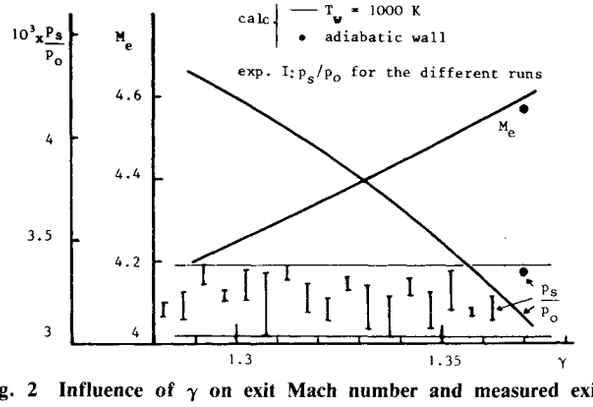

Fig. 2 Influence of γ on exit Mach number and measured exit pressure.

isentropic relations as well as the impact pressure distribution by the Rankine-Hugoniot relations.

The reduced impact pressure distribution p_t/p_o and the reduced number density distribution n/n_o along the jet axis have been calculated by this model and plotted as solid lines in Figs. 3 and 4, respectively. For comparison, similar distributions based on nozzle exit conditions consistent with a smaller value (1.33) of the specific heat ratio have been plotted in Figs. 3 and 4 as dotted lines and do not differ much from the preceding ones. Varying γ within the realistic range of values indicated above (1.36-1.38) would have resulted in nearly indistinguishable curves. Thus, in spite of the remaining uncertainty concerning γ, meaningful comparisons of predicted and measured values of Pitot pressure and density are possible.

Pilot Probe Measurements

The impact pressure was measured at different locations in the jet within the range of coordinates indicated above. The Pitot probe was usually moved from one place to another between successive runs. However, some measurements were duplicated to check reproducibility of results. The measured pressure p_t was reduced by the combustion chamber pressure p_o measured at the same time, which minimized the influence of unsteadiness of both p_t and p_o. No systematic variation of p_t/p_o vs time was observed. The external diameter of the Pitot probe was approximately 4 mm. Due to the shock detachment distance and to the nonuniformity of the flow, an error in the measured pressure might have occurred. It was confirmed that this error was less than 1%, even after accounting for rarefaction effects, and it was therefore neglected.

The bars represented in Fig. 3 indicate the minimum and maximum values of p_t/p_o recorded during one or more runs at different locations along the axis of the jet. Figure 3 includes a few results that were not actually obtained on the jet axis, but at some distance away from the jet axis. In that case, the measured values of p_t/p_o were multiplied by $p_t(0)/p_t(\theta)$ before plotting, the correcting factor being given by the above jet model. Only those data which required less than 15% correction were included in Fig. 3. Impact pressure distribution appears consistent with the proposed model within experimental uncertainty. It is worth pointing out that no fitting was introduced in the comparison.

Electron Beam Measurements

Although many investigators have used the electron beam fluorescence technique for gas density measurements and much work has been devoted to the method itself, this technique is far from being a straightforward one, especially when applied to rather unusual gases.

The number density in the investigated jet region ranged approximately from 10^{15} to 3×10^{16} mole/cm^3 and the temperature from 50 to 150 K, assuming isentropic expansion.

According to the estimation of Rebrov et al.,[5] it was assumed that the luminescence of the gas mixture in the selected wavelength range (3914 Å band of N_2) was due solely to the fast primary electrons of the beam.

The intensity of luminescence I is therefore proportional to the beam intensity i passing through the viewed volume. Due to elastic collisions with the gas molecules at relatively high density, beam broadening occurs and results in a variation of i that must be accounted for. As i was not directly measurable, it was simply assumed that it was proportional to the beam intensity i_c collected on the Faraday cup.

Under these hypotheses, the intensity of luminescence may be written as

$$I = k\, i_c \sum_i \{\alpha_i n_i / (1 + \sum_j (n_j / n(i,j)))\} \tag{4}$$

In the present analysis, the eventual variation of α_i and $n(i,j)$ with temperature has been neglected.

A systematic study of the spectra of different gases excited by high-energy electrons can be found in Ref. 6. With the exception of HCl, all gases in the present mixture were considered in Ref. 6 and only N_2, $C0_2$, and C0 exhibited significant emission in the wavelength range considered in the present work. The possible emission of HC1 was neglected. Quantitative information on the relative values of the emission cross sections of the different gases is difficult to get from Ref. 6, but may be obtained from work performed at the Institute of Thermophysics (Novosibirsk) on binary mixtures $N_2 + C0_2$ and $N_2 + C0$ and on pure N_2, $C0_2$, and C0.[7] In the absence of quenching, the luminescence originating from the different gases for given species densities is proportional to the coefficient α_i introduced above. Approximate values given by Ref. 7 are $\alpha_{N_2}/\alpha_{C0_2} = 4$ and $\alpha_{N_2}/\alpha_{C0} = 7$. Let us define

$$m = \left(\sum_i \alpha_i n_i\right) \Big/ (\alpha_{N_2} n_{N_2}) \tag{5}$$

where m denotes the ratio of total luminescence of the gas mixture in the absence of quenching to the fraction of that luminescence originating from nitrogen. Introducing the exhaust gas composition given in Table 1 yields $m = 1.63$. Obviously, m is equal to 1 under the conditions of air calibrations, since the air components other than nitrogen have negligible emissivity.

Concerning the quenching, a two-dimensional array $n(i,j)$ should be used. Unfortunately, little information on these constants is available in the literature, except for the quenching of N_2 emission by N_2 or other gases.[6,8] It was therefore decided to simplify Eq. (4) by using the same set of quenching densities for all emission processes, namely the set of quenching densities available for N_2 emission. This approximation is justified by the fact that N_2 emission remains the main emission process under the present conditions.

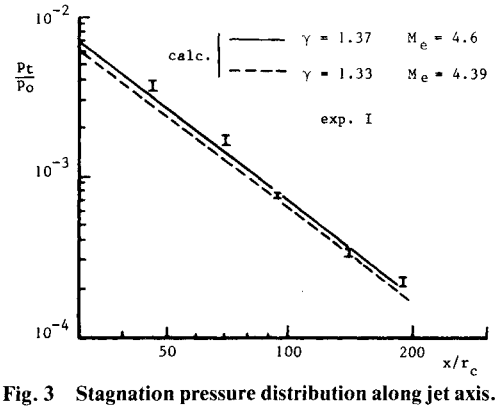

Fig. 3 Stagnation pressure distribution along jet axis.

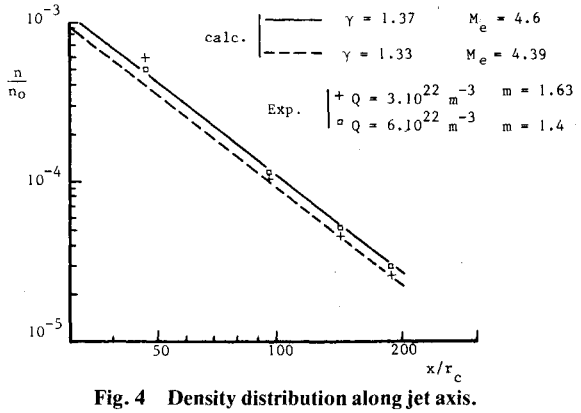

Fig. 4 Density distribution along jet axis.

Table 1 Gas composition under combustion chamber conditions

Gas	Mole fraction
$C0_2$	0.0738
C0	0.2154
H_2	0.1620
H_20	0.3127
N_2	0.0787
HC1	0.1474

Equation (4) may now be rewritten as

$$I = k\, i_c\, m\, c_{N_2}\, \alpha_{N_2}\, n/(1+n/Q) \qquad (6)$$

where Q is an overall quenching density defined by

$$1+n/Q = 1+\sum_j \{n_j/n(N_2,j)\} \text{ or } 1/Q = \sum_j \{c_j/n\,(N_2,j)\}$$

Reference 8 reports values of $n(N_2,N_2)$ ranging from 3.6×10^{16} to 6×10^{16} mole/cm^3, $n(N_2,0_2)$ equal to 3.6×10^{16} mole/cm^3. Reference 6 indicates that the quenching of N_2 emission by all gases investigated involves quenching densities larger than 2×10^{16} mole/cm^3 except quenching by $C0_2$, for which the range $5\times10^{15}-2\times10^{16}$ mole/cm^3 was proposed. Based on this information and on gas composition, two values were retained for Q:

1) A low value ($Q=3\times10^{16}$ mole/cm^3 for exhaust gas and 3.6×10^{16} mole/cm^3 for calibration in air) was calculated assuming a value of 10^{16} mole/cm^3 for quenching by $C0_2$ and 3.6×10^{16} mole/cm^3 for quenching by other gases.

2) A high value ($Q=6\times10^{16}$ mole/cm^3) based on a unique quenching density (6×10^{16} mole/cm^3) for all gases.

Electron beam measurements were performed at different locations in the jet. Local number density was obtained from Eq. (6), the constant k being obtained by another application of Eq. (6) to the preliminary calibration measurements.

The resulting axial density distribution is plotted in Fig. 4 for two hypotheses relative to m and Q. Since m acts as a multiplying factor for all the experimental points and Q acts only on those measurements where quenching is present (i.e., $X/r_c \leq 100$), their influence may be discussed separately. Local number density is reduced by the combustion chamber density n_o, based on $T_0=2400$ K, and on the experimental value of p_o. A few data obtained at a small distance away from beam axis have been plotted after a correction similar to the correction previously used for Pitot probe measurement.

Number density values obtained at large abscissa for $m=1.63$ fall somewhat below the values predicted by the model. Using $m=1.4$ gives a better agreement, which tends to indicate that the relative contribution of N_2 to luminescence is slightly larger than estimated.

When estimated using the low value of quenching density (3×10^{16} mole/cm^3 in the jet and 3.6×10^{16} mole/cm^3 for air calibration), the axial density profile exhibits significant curvature, which is consistent neither with the model nor with the Pitot pressure distribution. Using the high value of quenching density (6×10^{16} mole/cm^3 in the jet and for air calibration) strongly reduces the curvature.

Thus assuming $m=1.4$ and $Q=6\times10^{16}$ mole/cm^3 leads to axial number density distribution consistent both with the model and the Pitot pressure distribution. This is confirmed by Fig. 5, in which three axial Mach number distributions have been plotted as deduced from the model, from Pitot probe measurements, and from electron beam probe, respectively.

Because of the approximation introduced in the interpretation of electron beam data, and because of the uncertainty in T_0, the values of m and Q which lead to the most consistent results are not claimed to be the exact values of the physical quantities denoted by m and Q, respectively. But the fact that only small adjustments from the first physically realistic values of m and Q were required gives confidence in the possibility of using an electron beam probe in nonclassical situations.

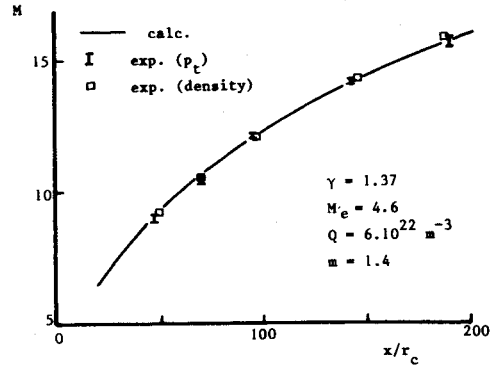

Fig. 5 Mach number distribution along jet axis.

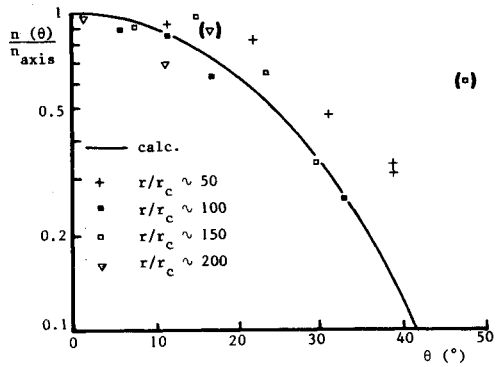

Fig. 6 Angular distribution of density.

The results of all density measurements performed in the jet have been plotted in Fig. 6 in a form which displays the angular distribution of density. Local density was deduced from the measurements, assuming $m=1.4$ and $Q=6\times10^6$ mole/cm^3 and reduced by the density calculated by the model on the jet axis for the same value of r. If both model and experiment were perfect, all data should fall on the solid line representative of Eq. (3). The two data in parentheses in Fig. 6 were taken outside the central part of the jet and therefore should not be considered for the comparison. Experimental scatter is important, but no systematic deviation from the model is evident.

Conclusion

The wall pressure measurement near the nozzle exit section is consistent with a value of γ approximately equal to 1.37, which indicates weak or zero vibrational relaxation of the exhaust gas.

The impact pressure distribution along the axis of the jet is consistent with the model described in Ref. 1, without any fitting.

The axial and angular density distributions deduced from electron beam measurements are consistent with the model and with the impact pressure distribution, provided some fitting is made for the relative contribution of N_2 to total luminescence and for the overall quenching density. Nevertheless, the optimal values found for these fitting parameters are close to the values predicted on the basis of physical considerations.

The possibility of using an electron beam probe in a gas mixture formed by the combustion products of solid propellant has been demonstrated. Further work with different gases at relatively high density is nevertheless desirable to get more precise information on emission and quenching cross sections.

Acknowledgment

The authors gratefully acknowledge the financial support of "Aérospatiale."

References

[1]Lengrand, J. -C., Allègre, J., and Raffin, M., "Underexpanded Freejets and their Interaction with Adjacent Surfaces," *AIAA Journal,* Vol. 20, Jan. 1982, pp. 27-28.

[2]Lengrand, J. -C., "Calcul de jets sous-détendus issus de tuyères supersoniques," Laboratoire d'Aérothermique du Centre National de la Recherche Scientifique, Meudon, France, Report 75-4, Dec. 1975.

[3]Brokaw, R. S., "Viscosity of Gas Mixtures," NASA TN-D 4496, April 1968.

[4]Boynton, F. P., "Highly Underexpanded Jet Structures, Exact and Approximate Calculations," *AIAA Journal,* Vol. 5, Sept. 1967, pp. 1703-1705.

[5]Rebrov, A. K., Karelov, N. V., Sukhinin, G. I., Sharafutdinov, R. G., and Lengrand, J. C., "Electron Beam Diagnostics in Nitrogen: Secondary Processes, *Proceedings of the 12th RGD Symposium, Progress in Aeronautics and Astronautics,* Fisher, S.S., ed., Vol. 74, Part II, 1981, pp. 931-945.

[6]Rothe, D. E., and McCaa, D. J., "Emission Spectra of Molecular Gases Excited by 10 keV Electrons," Cornell Aeronautical Laboratory, Inc., Buffalo, N.Y., CAL No. 165, Dec. 1968.

[7]Sharafutdinov, R. G., Institute of Thermophysics, Novosibirsk, private communication, June 1981.

[8]Muntz, E. P., "The Electron Beam Fluorescence Technique," AGARD No. 132, Dec. 1968.